Interval Approach to Robust Bounded-Error Estimation of Corrupted Experimental Data

S.I. Kumkov *

* *Institute of Mathematics and Mechanics, Ural Branch, Russian Academy of Sciences, Russia, Ekaterinburg, S.Kovalevskaya str. 16, 620219 (e-mail: kumkov@imm.uran.ru).*

Abstract:
Interval analysis has been successfully applied to parameter and state estimation form noisy experimental data. However, obtaining efficient set estimators which are robust to outliers is still very difficult. This paper introduces new robust parameter and state estimation techniques in a bounded-error context in the presence of outliers. Several examples are provided concerning guaranteed parameter estimation of some chemical processes and the state tracking of aircrafts.

Keywords: Corrupted data, outliers, dependence, parameters, estimation, procedures, practical problems.

1. INTRODUCTION

In practical experiments there are situations where the measurement error has a chaotic character and some measurements seem to be outliers. For example, Fig.1 illustrates the case with multiple chaotic outliers (crosses) mainly of positive sign; they have suspiciously large deviations from the anticipated region (marked in dashes). The correct measurements are marked with black circles, theoretically given dependence is the exponent.

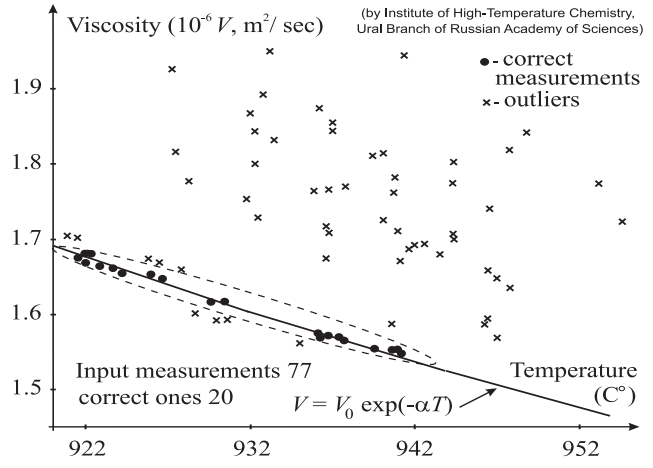

Fig. 1. Electrolyte viscosity in an electro–chemical process as a function of temperature

Figure 2 shows the case where the measurements include corruptions both in the argument (K_{CU}, impact viscosity) and in the measured values (K_{1C}, static fracture resistance). Moreover, the form of the dependence changes in different intervals (1, 2 and 3) of the argument and the boudaries of these intervals can be marked approximately. Both ordinary measuring errors and outliers are present. So, an attempt to explain all samples by a line (in solid) is not satisfying.

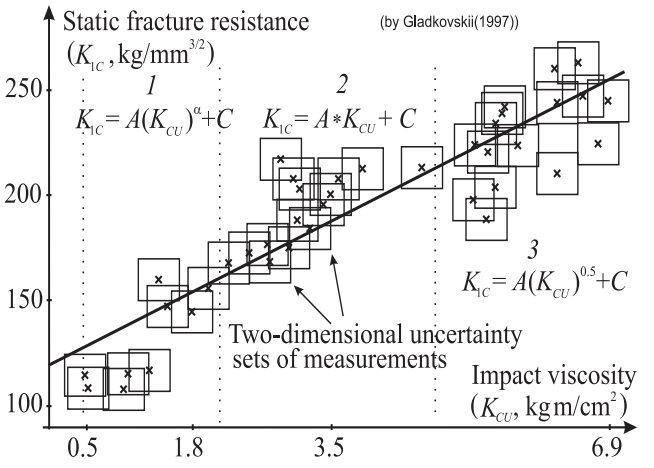

Fig. 2. Corrupted sample of measurements in investigation of metal stiffness

Usually in presence of outliers, standard regression and statistical methods to perform parameter estimation are unsatisfying for several reasons. First, obtaining the probability density function of measurement noise and, *a fortiori*, of outliers is difficult. Special investigations show that, as a rule, distribution of corrupted measurements is not Gaussian (Fig.3). Second, this is especially difficult when few measurements are available only, and the input sample is short (see, Section 3). Third, outliers may lead to some bias (shift) in measurement noise. Fourth, in absence of information on density functions, it is impossible to speak about any confidence probabilities and confidence intervals. See, also, reasons for foundation of interval analysis approaches in Jaulin, et al. (2001), Milanese, et al. (1996), Hansen (2004).

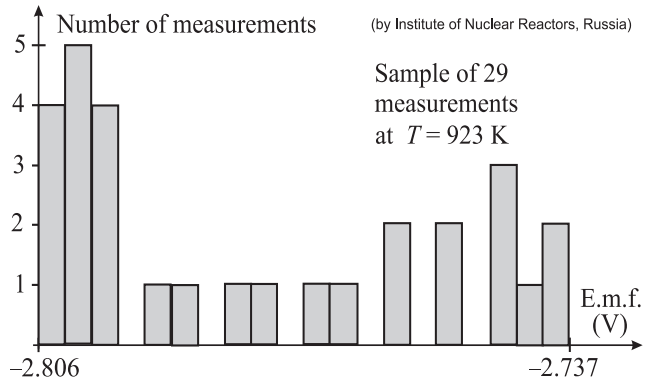

Fig. 3. Histogram of electromotive force measurements versus voltage; a molten electrolyte in a nuclear reactor

2. INTERVAL APPROACH

The following input information is considered.
1. The dependence under investigation is described by some *function* $y = f(x,p)$ or a *system* $dy/dt = f(t,p)$ of differential equations (in the case of a dynamical process) with the main argument x and a vector p of parameters to be estimated.
2. Several *models of corruption* of measurements may be chosen. In practice the following ones are widely used

$$\begin{array}{l} a)\ y = y^* + e, \quad b)\ y = y^* + \delta y^*, \\ c)\ y = y^* + \delta y^* + e, \\ |e| \le e_{\max},\ |\delta| \le \delta_{max}, \end{array} \tag{1}$$

where y is a corrupted measurement; y^* is the noise–free measured quantity; e is the *absolute* measurement error independent on the measured value and bounded in modulus; δ is the *relative* measurement error bounded in modulus and providing the error component proportional to the measured value. To illustrate the elaborated interval approach to estimation, below we shall only consider the Model a).
3. A sample of the length N of corrupted measurements is given

$$\{y_n\},\ n = 1, \dots, N. \tag{2}$$

The following interval procedures A ÷ G are considered.
A) Around each measurement y_n in (2), the interval *uncertainty set* (USM) $H_n = [\underline{h}_n, \overline{h}_n]$ is built and has the lower $\underline{h}_n$ and upper $\overline{h}_n$ bounds

$$\underline{h}_n = y_n - e_{\max},\ \overline{h}_n = y_n + e_{\max}. \tag{3}$$

Definition 2.1. *A curve $y = f(x,p)$ of a given type is called* admissible *with respect to a collection of* USMs $H_i, \dots, H_l, \dots, H_m$ *of several indices* $\{i, \dots, l, \dots, m\} \in 1 \div N$ *if it* passes *through all of them*

$$y = f(x,p) :\ f(x_k,p) \in H_k,\ k \in \{i, \dots, l, \dots, m\}. \tag{4}$$

Definition 2.2. *The set $G_{i\dots l\dots m}$ of values of the parameter vector corresponding to an admissible curve is called the admissible* partial informational set (PINS) *of parameters if*

$$G_{i\dots l\dots m} = \{p :\ f(x_k,p) \in H_k,\ k \in \{i, \dots, l, \dots, m\}\}. \tag{5}$$

Definition 2.3. *The set I of values of the parameter vector corresponding to a collection of admissible curves is called the* informational set *of parameters* (or the set-membership)

$$I = \{p :\ f(x_k,p) \in H_k,\ k = 1, \dots, N\}. \tag{6}$$

Definition 2.4. *The collection Tb of admissible curves is called the* tube *of dependence*

$$\begin{array}{l} Tb = \{y(x_k,p) :\ y(x_k,p) \in H_k, \\ \qquad p \in I(p),\ \ x_k, k = 1, \dots, N\}. \end{array} \tag{7}$$

Remark 2.1. *Similar definitions can be given for the case of estimation of parameters or states of a dynamical system described by differential equations.*

Below for specifity of description, elaborated interval procedures for parameter estimation are illustrated on an example of a linear function $y(x,p)$ with a two-dimensional vector $p = (a,b)$ of parameters, and the function is given on an interval of an argument $[x] = [\underline{x}, \overline{x}] \in \mathbf{R}$ with a grid of values $\{x_n\}, n = 1, \dots, N$

$$y(x_n,a,b) = a + bx_n,\ \underline{x} = x_1, \dots, x_n, \dots, \overline{x} = x_N. \tag{8}$$

B) Construct the collection of "pairwise" $\{G_{ik}\}$ partial informational sets (PINS). Since of properties of function (8), each pair H_i–H_k of USMs defines exact parallelogram PINS G_{ik} on the basis of marginal and intermediate dependencies and corresponding points (a_1,b_1)–(a_4,b_4) (Fig.4)

$$\begin{array}{l} G_{ik} = \{a,b : a + bx_i \in H_i \ and\ a + bx_k \in H_k\}, \\ \qquad for\ i,k = 1, \dots, N,\ k > i. \end{array} \tag{9}$$

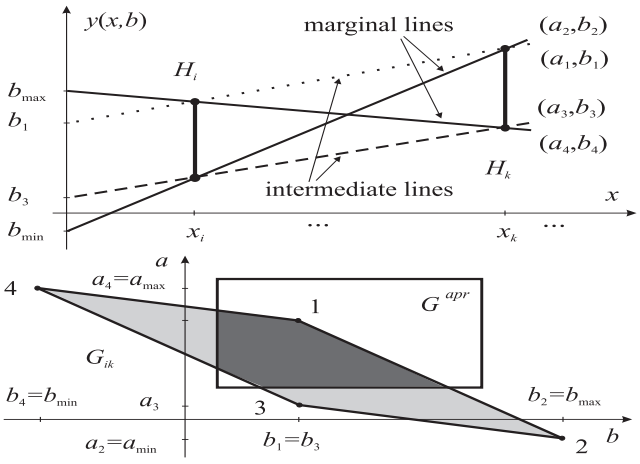

Fig. 4. A pair of USMs and its PINS of parameters

Note that this technique is rather flexible and allows one to take into account any *a priori* information on possible values of the parameters. Let some *a priori* rectangle $G^{apr}(a,b)$ be given in lower part in Fig.4). So, it is possible to enhance the result of estimation (in dark gray) by intersecting the PINS G_{ij} with $G^{apr}(a,b)$.

C) Construct the informational set I of parameters a,b for a *consistent* sample (2) is performed by intersection of PINS (Fig.4, parallelograms in light gray) by some standard operation of intersection of convex sets

$$I = \bigcap_{i,k=1,\dots,N,\ k>i} G_{ik} = \bigcap_{i\equiv 1,\ k=2,\dots,N} G_{1k}. \tag{10}$$

Note that the latter relation in this formula is valid for a *linear dependence* of function (8) on parameters a,b.

Moreover, in this case, the informational set is a convex polygonal with linear boundaries between its apices.

D) Construct the tube $Tb(x)$ of admissible dependences consists in calculation of the collection of its lower $\underline{Tb}(x)$ and upper $\overline{Tb}(x)$ frontier points for each value of the argument $x_k,\ k = 1, \ldots, N$,

$$\begin{aligned} \underline{Tb}(x_k) &= \min_{(a,b)\in I} \{a + bx_k\}, \\ \overline{Tb}(x_k) &= \max_{(a,b)\in I} \{a + bx_k\}. \end{aligned} \tag{11}$$

For the *linear function* (8), the tube upper (lower) frontiers on intervals $[x_k, x_{k+1}$ are lines connecting corresponding upper (lower) edges of the cross–sections $[\underline{Tb}(x_k), \overline{Tb}(x_k)]$ and $[\underline{Tb}(x_{k+1}), \overline{Tb}(x_{k+1})]$.

E) The output data for the user consist of tube (11), informational set (10), its bounding intervals $[a] = [\underline{a}, \overline{a}]$ and $[b] = [\underline{b}, \overline{b}]$, and the central point (a_{cntr}, b_{cntr})

$$\begin{aligned} &\underline{a} = arg\{\min a \in I(a,b)\},\ \overline{a} = arg\{\max a \in I(a,b)\}, \\ &\underline{b} = arg\{\min b \in I(a,b)\},\ \overline{b} = arg\{\max b \in I(a,b)\}, \\ &a_{cntr} = (\underline{a} + \overline{a})/2,\quad b_{cntr} = (\underline{b} + \overline{b})/2. \end{aligned} \tag{12}$$

F) The suggested estimator A–E is arranged with special algorithms, which allow one to investigate structure of a corrupted sample in the case when the informational set (10) of the whole sample does not exist, i.e., is empty. Let for the given constraint $e_{\max}$ in (1) onto value of the corruption the input sample (2) it be *inconsistent*. Corresponding algorithms and software had been elaborated on the basis of the graph theory Kumkov (2009) that divide such a sample *inconsistent in the whole* into consistent subsamples of various length. For example, if a single outlier, say with number j, is present, then all collection of PINSs of the form $G_{jk},\ k = 1, \ldots, N,\ k \neq j$ has empty pair-wise intersections. For a researcher the most interest is in a subsample of the maximal length.

G) The suggested estimator A–E allows one to introduce special procedure for estimation of the *actual level* of corruption in the given input sample (2). Let for the given constraint $e_{\max}$ in (1) onto value of the summary corruption the input sample (2) be *inconsistent* in spite of absence of "evident" outliers. It this case by increasing a level of the constraint $e_{\max}$ we obligatory come to the situation when for some *critical* level $e^*_{\max}$ the informational set becomes *non-empty* and consists of only one point $I(a,b) = (a^*, b^*)$. Such a value $e^*_{\max}$ is an estimate *from below* of the actual level of corruptions in measurements of the input sample. In the case of initially consistent sample, the outer estimate (from below) $e^*_{\max}$ of the actual level of corruptions is found similarly by *decreasing* the constraint $e_{\max}$ from its initial value.

Remark 2.2. *The suggested estimator* A–E *exploits the idea of the* inclusion functions (*described in* Jaulin, et al. (2001), Milanese, et al. (1996), Hansen (2004), Shary (2011)) *and allows one to build constructive procedures in various practical problems* Gladkovskii (1997), Kumkov (2010a), Kumkov (2010b), Kumkov (2009) *both with linear describing function and nonlinear functions that can be reduced to a linear ones* (see, e.g., State Standard (2003)). *In particular, the estimator was effectively applied to estimation of coefficients in polynomials or polynomial representations of complicated nonlinear functions.*

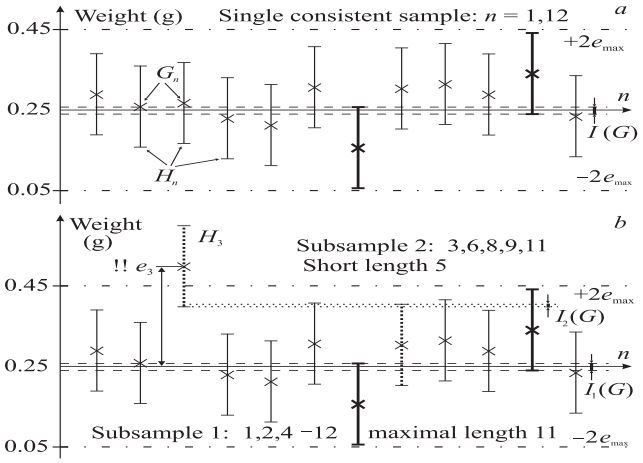

Fig. 5. Estimation of a weight; consistent (a) and inconsistent (b) samples

3. APPLICATION OF ELABORATED ALGORITHMS TO PRACTICAL PROBLEMS

Consider now several practical problems solved on the basis of the described interval approach.

Example. 3.1. Estimation of a physical constant. This problem is typical in metrology. The describing function is an unknown constant G^*. Model data and results of estimation are given in Fig.5. The true weight is 0.25 g, the constraint on the bound on corruption is $e_{\max} = 0.1$ g, the sample contains corrupted measurements $\{G_n\}$, $n = 1, 12$.

In version *a*, it is seen that the summary corruption (a measurement error + chaotic component) does not exceed the constraint $e_{\max}$. The informational set $I(G)$ in not empty since all uncertainty intervals H_n of measurements have nonempty intersection. So, the sample is consistent and has the maximal length of 12 measurements.

In version *b*, the third measurement has been simulated with the summary corruption $e_3 > 2e_{\max}$. As a result, the sample is inconsistent in the whole, and the estimator outputs two consistent (in itself) subsamples. The first subsample contains measurements 1,2,4 – 12 and has the maximal length of 11. The second subsample is generated by the third corrupted measurement. Note that application of a statistical approach recommended by State Standard (2003) does not "sense" such fragmentation of the input sample since of enlarged corresponding value of standard deviation (i.e., of large σ).

Example. 3.2. Estimation of a chemical process. The real process Mikushuna, et. al (2010) of conversion $Cnv(m)$ versus the mass m of nano-catalyst is described by the simplest linear function with one parameter B (Fig.6). Corruptions are both in measurements of mass m (the constraint is $e^m_{\max} = 2$ mg) and conversion Cnv (the initial constraint is $e^{init}_{mes} = 1.00$ %). There are only 3 actual measurements; the first "measurement" (and its USM H_1) is identically equal to zero by the physical sense of the experiment. Here, the uncertainty sets $H_i,\ i = 2, 3, 4$ of measurements are *non-intersecting* rectangles. Simplicity of the model allows one to define partial informational intervals G_2, G_3, and G_4 (Fig.7) by apices of USMs.

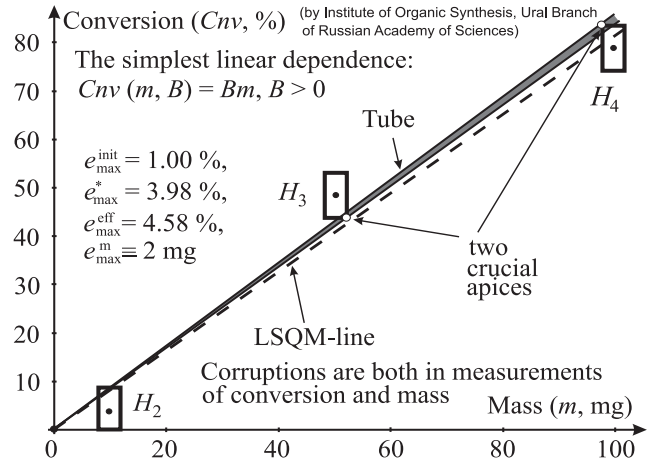

Fig. 6. Investigation of conversion by nano-catalyst

For the initial e^{init}_{mes} value of constraint the sample is inconsistent, i.e., there is no any of the parameter such that the model output passes through all H_1, H_2, H_3, and H_4. The critical value (by procedure G described above) is $e^*_{mes} = 3.98$ %, and the informational set is a point $I(B, e^*_{mes}) = B^*$ (Fig.7a). Having increased the constraint up to an *effective* value $e^{eff}_{mes} = 4.58$ %, we obtain enlarged partial informational intervals G_2, G_3, and G_4 (Fig.7b) with non-empty informational interval $I(B, e^{eff}_{mes})$.

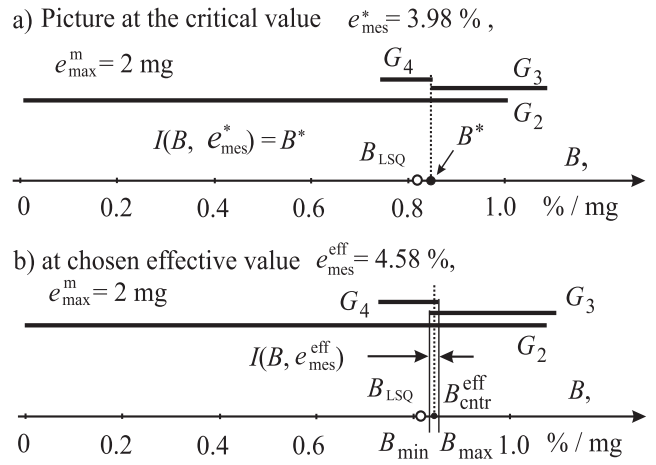

Fig. 7. Nano-catalytical conversion; estimation of informational interval of coefficient B

Remark 3.1. *Increasing the constraint e_{mes} from the critical value e^*_{mes} up to some effective value e^{eff}_{mes} is similar to the choice of desirable value of* confidence probability *and corresponding* confidence interval *in the statistical approach* State Standard (2003).

Example. 3.3. Investigation of dependence of ionic conductivity (Fig.8 and Fig.9). Here, real ionic conductivity $S(x)$ is measured versus the argument x depending on temperature. The describing function is nonlinear $S(x, V, \alpha, BG) = V \exp(\alpha x) + BG$. The sample $\{S_k = S(x_k)\}$, $k = 1, 8$, was given; the experiment Sutto, et al. (2002) had been performed very carefully, and there are no outliers in the sample. The following estimation of the admissible set of parameters is performed. By shifting the background parameter BG to the left-hand side and by standard logarithmic operation, the following linear function of a new variable $y = Ln\big(S(x) - BG\big)$ and with a new parameter LnV is obtained

$$y(x, LnV, \alpha) = Ln\big(S(x) - BG\big) = LnV + \alpha x. \qquad (13)$$

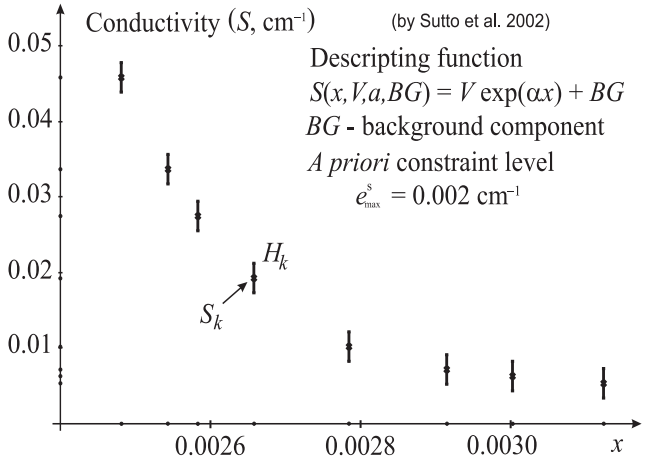

Fig. 8. Investigation of the chemical dependence

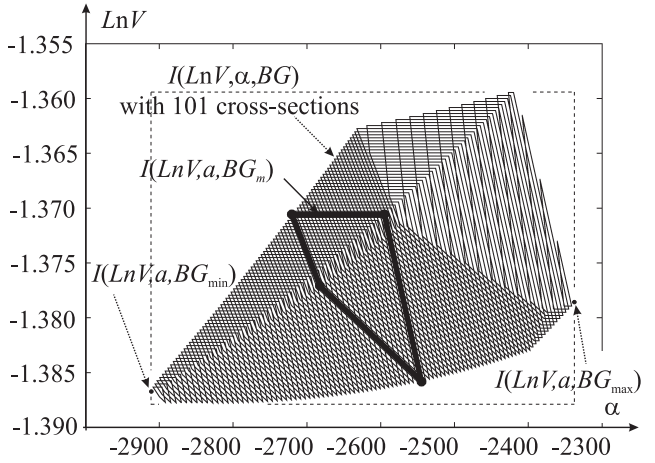

Fig. 9. Informational set of parameters for the chemical dependence

Further, a grid $\{BG_m\}, m = 1, M$, with reasonable step δ_{BG} was introduced on some initial *a priori* known interval $[BG]^{init}$. Centering the sample $\{S_k\}$ by a node BG_m, we obtain a transformed collection of measurements $\{y_{km}\}$, $k = 1, \ldots, 8$, with linear describing function (13). Apply now the interval approach to this collection. If the triple LnV, α, BG_m is admissible, then we obtain *non-empty* informational set $I(LnV, \alpha, BG_m)$ of parameters; in Fig.9 it is shown as a polygonal projection (in thick contour) onto the plane $LnV \times \alpha$. Otherwise, i.e., if the informational set is empty, such a triple is not admissible.

Implementing these operation with necessary adjusting the grid $\{BG_m\}$ and its step, the admissible interval $[BG] = [0.002996, 0.005757]$ cm^{-1} of parameter BG with a fine step $\delta_{BG} = 0.00002761$ cm^{-1} and with 101 nodes has been found. Guarantee of estimation of the BG interval is provided by adjusting the grid position always around admissible values of the parameter. Since the grid is one-dimensional, this search is faster than universal sophisticated procedure SIVIA with parallelotops Jaulin, et al. (2001).

Simultaneously, corresponding collection of the non-empty informational sets $I(LnV, \alpha, BG_m)$ in projection onto the plane $LnV \times \alpha$ has been constructed (Fig.9). In its essence, this collection is a collection of cross-sections of the three-dimensional informational set $I(LnV, \alpha, BG)$ of admissible values of parameters in the space $LnV \times \alpha \times BG$. In Figure 9 the edge-points, i.e., the marginal point-wise informational sets $I(LnV, \alpha, BG_{\min})$ and $I(LnV, \alpha, BG_{\max})$ are marked by black circles. The rectangle in dashes shows the minimal outer interval estimate of the set.

Example. 3.4. Fast estimation of velocity and heading of an aircraft in an air traffic control system (ATC system). An aircraft motion (Fig.10) is observed in the coordinate plane $x \times z$ of an ATC system. The sample of aircraft positions are measured at three instants (t_i, x_i, z_i), $i = 1, 2, 3$. By properties of measuring radar system, corruption in each measurement is assumed to be a round-wise with a constraint r; so, the uncertainty set $H_i(x, z)$ of each measurement is a circle. Direct motion of the aircraft with a constant velocity on the interval $[t_1, t_3]$ is described by expressions where x_0, z_0 are initial coordinates from H_1 at the initial instant $t_1 = 0$.

$$\begin{aligned} &x(t, V, \psi) = x_0 + tV\cos\psi, \\ &z(t, V, \psi) = z_0 + tV\sin\psi, \\ &\psi(t) \equiv \psi_{const},\ V(t) \equiv V_{const}, \end{aligned} \tag{14}$$

In Fig.10, the image of true trajectory is shown in thick, the true positions of the aircraft on this trajectory at t_1, t_2, t_3 are marked by white circles. It is necessary to estimate the aircraft velocity and heading on this time interval and it is desirable to have a fast algorithm for computations in the real-time mode.

Consider possible pairs of USMs H_1–H_2, H_1–H_3, and H_2–H_3. Using model (14) and the circle form of USMs, the possible outer interval estimate of the velocity $[V]_{ij} = [\underline{V}_{ij}, \overline{V}_{ij}]$ is evidently calculated for each pair

$$\begin{aligned} &\underline{V}_{ij} = (d_{ij} - 2r)/(t_j - t_i), \\ &\overline{V}_{ij} = (d_{ij} + 2r)/(t_j - t_i), \\ &d_{ij} = sqrt\big((x_j - x_i)^2 + (z_j - z_i)^2\big). \end{aligned} \tag{15}$$

Similarly, the possible outer interval estimate of the heading angle $[\psi]_{ij} = [\underline{\psi}_{ij}, \overline{\psi}_{ij}]$ is calculated for each pair as angles of corresponding outer marginal tangents (Fig.10) of a considering pair H_i–H_j. As an example, marginal values $\underline{\psi}_{13}$ and $\overline{\psi}_{13}$ of heading for the pair H_1–H_3 are also shown in Fig.10.

The outer partial informational set $\mathbf{G}_{ij}(V, \psi) = [\underline{V}_{ij}, \overline{V}_{ij}] \times [\underline{\psi}_{ij}, \overline{\psi}_{ij}]$ is shown in Fig.11a by the rectangle. Here also, boundary of the exact partial informational set $G_{ij}(V, \psi)$ of these parameters is marked by a dash curve (this boundary can be computed by special complicated formulas and is out of consideration). The outer estimate $\mathbf{I}(V, \psi)$ of the informational set is built by intersection of outer partial informational sets $\mathbf{G}_{12}(V, \psi)$, $\mathbf{G}_{13}(V, \psi)$, and $\mathbf{G}_{23}(V, \psi)$ (Fig.11b, a rectangle in gray). As a point-wise estimate, the central point (white circle) of the set $\mathbf{I}(V, \psi)$ is given for the user.

Example. 3.5. Estimation of an aircraft motion in altitude in an ATC System (Fig.12). Here, real measurements of the aircraft altitude come with a random time step. The sample is accumulated and processed in the *sliding*

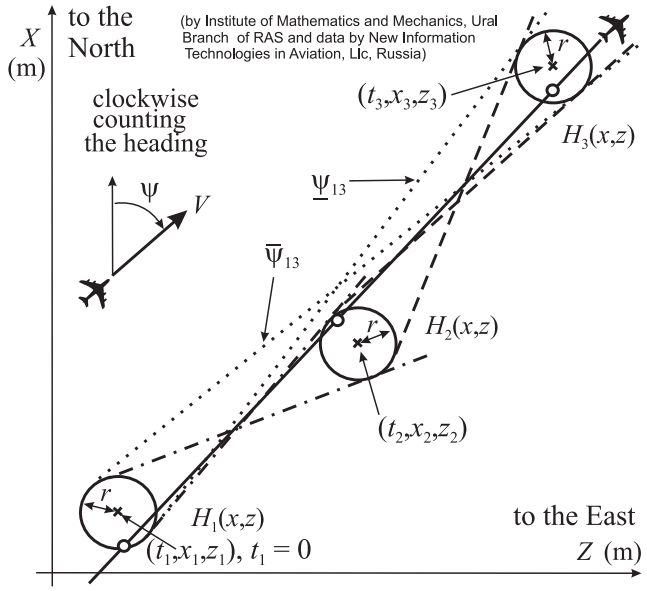

Fig. 10. Measurements of aircraft motion

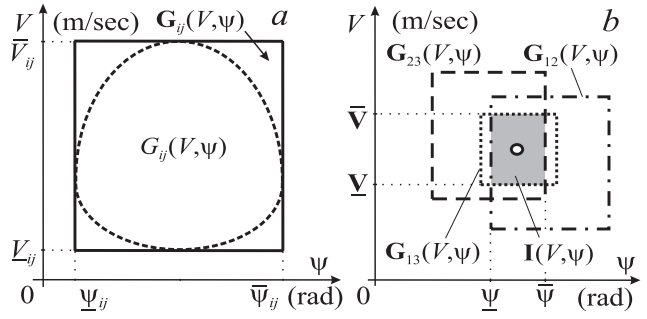

Fig. 11. Informational set of aircraft velocity and heading

window of 5 measurements. Constraint on value of the summary corruption is $\delta_y = 50$ m (typical for the GPS altitude measurements for a fast moving aircraft). Incoming corrupted measurements $\{y_i\}$, $i = 1, 2, ...$ are marked with black circles. Uncertainty intervals H_i of measurements are drown by thin vertical segments. The aircraft motion in altitude is described as follows:

$$\begin{aligned} &y(t, V) = y_0 + V_y t, \\ &y_0 \in [\underline{y}_0, \overline{y}_0], \\ &V_y(t) \equiv V_y^{const} \in [\underline{V}_y, \overline{V}_y]. \end{aligned} \tag{16}$$

Here, V_y is the vertical velocity from the given uncertainty interval $\underline{V}_y = -1.5$ m/sec, $\overline{V}_y = 1.5$ m/sec; $y_0 \in H_1$ is the initial position at $t_1 = 0$ from the uncertainty interval equal to the uncertainty set H_1 of the first measurement at the beginning of processing the incoming information.

Under mentioned uncertainty conditions, it is necessary to estimate the aircraft track, i.e., the tube of admissible aircraft trajectories in altitude. The interval approach to estimation considered above is implemented by the following procedures.

At the initial instant $t_1 = 0$ the algorithms start and put in the uncertainty set H_1 as a set of possible initial positions y_0. Having accumulated measurements $y_1 - y_6$ as the input sample, the *forward–backward propagation* of constraints is applied (see, e.g., Jaulin, et al. (2001)). Using the model of motion (16), the boundaries of each USM are forecasted in

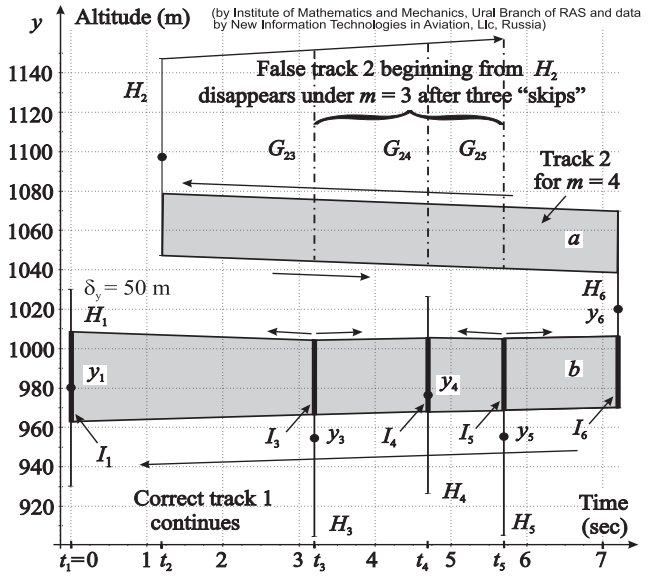

Fig. 12. Estimation of aircraft altitude; partition into two inconsistent subsamples and elimination of the outlier

the forward and backward time that gives corresponding forecast sets G_{ij}. Here, the first index i is the number of the instant from which forecast is begun, the second index j corresponds to the instant of the forecast.

The process is illustrated by prognosis of the USM H_2 (Fig.12, in the upper part). Thin forward and back arrows point the direction of the forecast. Each forecast set is intersected with corresponding USM H_j. By a special rule of the ATC technology, a measurement y_i is regarded as *inadmissible outlier* if its forecast sets G_{ij} for $j = i + 1, i + 2, \ldots, i + m$ successively have empty intersections with all corresponding USMs H_{i+1}, $H_{i+2} \div H_{i+m}$. Here, m is a constraint onto the number of *skipped* measurements usually chosen in practice as $m = 3 \div 4$.

Application of the forward–backward propagation of constraints gives the following results (Fig.12). Under constraint $m = 3$, the second measurement y_2 was classified as an outlier, since its forecast sets G_{23}, G_{24}, and G_{25} have empty intersections with USMs H_3, H_3, and H_5. So, after 3 skips the possible false track 2 is eliminated. In contrast, the first measurement (together with measurements 3,4,5, and 6 that were accumulated in the sliding window with the length of 5 measurements) generates authentic track 1. Under described conditions of uncertainty, the track 1 is represented by the *tube* of the admissible aircraft trajectories in altitude (Fig.12, lower part, the tube b in gray). Cross-sections I_1, I_3 – I_6 of this tube are shown in thick vertical segments. These are desirable state estimates of the aircraft altitude at the measuring instants.

Note one interesting detail. If the constraint onto number of skipped measurement is given as $m = 4$, the USM H_6 of the sixth measurement will have non-empty intersection with the possible forecast set G_{26}. As a result, the outlier y_2 will generate a *parallel* track 2 (Fig.12, upper part, the tube b in gray). But later, such a track will be merged by the actual one. These situations are typical in the air traffic control systems during aircrafts tracking using the radar or GPS information.

4. CONCLUSION

Considered interval approach to estimation of parameters for dependences and dynamical processes is effective under the presence corruptions in noised experimental information. As an alternative, the approach allows one to find estimates in the case of uncertainty of probability characteristics of possible measuring errors in the input data.

ACKNOWLEDGEMENTS

The work was supported by the RFBR grants, projects nos. 10–01–96006 and 11–01–12088

REFERENCES

S.V. Gladkovskii and S.I. Kumkov. Application of Approximation Methods to Analysis of Peculiarities of Break-up Process and Forecasting Fracture Resistance of High Strength Steel. *Mathematical simulation of systems and processes*, Collection of Scientific Works. The Perm State University, Perm, Russia, no. 5, pages 26–34, 1997.

E. Hansen and G.W. Walster. Global Optimization using Interval Analysis. Marcel Dekker, Inc., New York, 2004.

L. Jaulin, M. Kiffer, O. Didrit, and E. Walter. Applied Interval Analysis. Springer, London, 2001.

S.I. Kumkov. Procession of Experimental Data on Ionic Conductivity of Molten Electrolyte by the Interval Analysis Methods. *Rasplavy*, no. 3, pages 79–89, 2010.

S.I. Kumkov and A.A. Fedotov. Interval Estimation of Aircraft Motion Parameters under Conditions of Strong Corruptions in Measurements. *Avtomatika i Telemekhanika*, no. 2, pages 112–127, 2010.

S.I. Kumkov. Elaboration of a Russian–ISO Standard for Processing Measured Information under Conditions of Uncertainty of Corruptions and Small Number of Measurements (by Methods of Interval Analysis). http://www.ict.nac.ru/interval/Conferences/Interval-06

S.I. Kumkov and S.G. Pyatko. Aircraft Motion Estimation under Conditions of Uncertainty. *IFAC online Journal on Automatic Control in Aerospace*, 2010, paper AS09005.

Yu.V. Mikushina, A.B. Sishmakov, et. al. Activated Carbon and Carbon–Oxide Composite Materials. *Journ. Applied Chemistry*, V. 83, iss. 2, pages 308–312, 2010.

M. Milanese, J. Norton, H. Piet-Lahanier, and E. Walter (eds.) Bounding Approaches to System Identification. Plenum Press, New York, 1996.

S. Shary. Finite–Dimensional Interval Analysis. Electronic Book, 2011. http://www.nsc.ru/interval/Library/InteBooks/SharyBook.pdf

State Standard. R 40.2.028–2003. Recommendations on Definition of Calibration Characteristics. Gosstandart, Official Edition, Moscow, 2003.

T.E. Sutto, H.C. De Long, and P.C. Trulove. Physical Properties of Substituted Imidazolium Based Ionic Liquids Gel Electrolytes. *Zeitschrift fur Naturforschung A*, 2002. Vol.57, no. 11. pp.839–846.